0026-895X/10/7803-366–375$20.00
MOLECULAR PHARMACOLOGY
Vol. 78, No. 3
65490/3617059
Mol Pharmacol 78:366–375, 2010
Printed in U.S.A.

Molecular Determinants for Competitive Inhibition of $\alpha4\beta2$ Nicotinic Acetylcholine Receptors

Patricio Iturriaga-Vásquez, Annalisa Carbone, Olimpo García-Beltrán, Phil D. Livingstone, Philip C. Biggin, Bruce K. Cassels, Susan Wonnacott, Gerald Zapata-Torres, and Isabel Bermudez

Department of Chemistry, Faculty of Sciences (P.I.-V., O.G.-B., B.K.C.) and Department of Inorganic and Analytical Chemistry, Faculty of Chemical and Pharmaceutical Sciences (G.Z.-T.), University of Chile, Santiago, Chile; School of Life Sciences, Oxford Brookes University, Oxford, United Kingdom (A.C., I.B.); Department of Biology and Biochemistry, University of Bath, Bath, United Kingdom (P.D.L., S.W.); and Department of Biochemistry, University of Oxford, Oxford, United Kingdom (P.C.B.)

Received April 9, 2010; accepted June 14, 2010

ABSTRACT

The Erythrina alkaloids erysodine and dihydro-β-erythroidine (DHβE) are potent and selective competitive inhibitors of $\alpha4\beta2$ nicotinic acetylcholine receptors (nAChRs), but little is known about the molecular determinants of the sensitivity of this receptor subtype to inhibition by this class of antagonists. We addressed this issue by examining the effects of DHβE and a range of aromatic Erythrina alkaloids on [^{3}H]cytisine binding and receptor function in conjunction with homology models of the $\alpha4\beta2$ nAChR, mutagenesis, and functional assays. The lactone group of DHβE and a hydroxyl group at position C-16 in aromatic Erythrina alkaloids were identified as major determinants of potency, which was decreased when the conserved residue Tyr126 in loop A of the $\alpha4$ subunit was substituted by alanine. Sensitivity to inhibition was also decreased by substituting the conserved aromatic residues α4Trp182 (loop B), α4Tyr230 (loop C), and β2Trp82 (loop D) and the nonconserved β2Thr84; however, only α4Trp182 was predicted to contact bound antagonist, suggesting α4Tyr230, β2Trp82, and β2Thr84 contribute allosterically to the closed state elicited by bound antagonist. In addition, homology modeling predicted strong ionic interactions between the ammonium center of the Erythrina alkaloids and β2Asp196, leading to the uncapping of loop C. Consistent with this, β2D196A abolished sensitivity to inhibition by DHβE or erysodine but not by epierythratidine, which is not predicted to form ionic bonds with β2Asp196. This residue is not conserved in subunits that comprise nAChRs with low sensitivity to inhibition by DHβE or erysodine, which highlights β2Asp196 as a major determinant of the receptor selectivity of Erythrina alkaloids.

Introduction

Nicotinic acetylcholine receptors (nAChRs) composed of $\alpha4$ and $\beta2$ subunits are the most prevalent subtype expressed in the mammalian brain, where it constitutes the high-affinity binding site for nicotine (Cassels et al., 2005). It belongs to the Cys loop ligand-gated ion channel family that also includes the muscle nAChR, γ-aminobutyric acid receptors type A and C, glycine receptors, and serotonin type 3 receptors (Taly et al., 2009). By analogy to the muscle nAChR, the $\alpha4\beta2$ nAChR is thought to have two agonist binding sites that lie at the interface between an $\alpha4$ subunit and a $\beta2$ subunit. Several highly conserved aromatic amino acid residues contribute to the acetylcholine (ACh) binding site, and they are grouped into six noncontiguous sequences, referred to as loops A, B, and C (the principal component within the $\alpha4$ subunit) and D, E, and F (the complementary component within the $\beta2$ subunit). The conserved residues in the muscle nAChR are α1Tyr93 (loop A), α1Trp149 (loop B), α1Tyr190 and α1Tyr198 (loop C), and γTrp55 and δTrp57 (loop D) (Unwin, 2005). The fifth subunit in the $\alpha4\beta2$ nAChR is an accessory subunit because it does not directly contribute to the binding site and can be another $\beta2$ subunit [i.e., $(\alpha4\beta2)_2\beta2$], $\alpha4$ subunit [i.e., $(\alpha4\beta2)_2\alpha4$], or $\alpha5$ subunit [i.e., $(\alpha4\beta2)_2\alpha5$] (Kuryatov et al., 2008). $\alpha4\beta2$ nAChRs are therapeutic targets for modulation of pain and brain pathologies, such as Alzheimer's and Parkinson's diseases, depression,

This work was supported by the National Foundation of Science and Technology [Grant 11060502]; the Millenium Scientific Initiative [Grant P05-001-F]; a Oxford Brookes University postgraduate scholarship; a Research Councils UK Fellowship; the Wellcome Trust [Grant 083547]; the Start-up Project [DI 2006 INI 06/03-2]; and the Bicentenary Project for Science and Technology, National Commission for Science and Technology 2004.

Article, publication date, and citation information can be found at http://molpharm.aspetjournals.org.

doi:10.1124/mol.110.065490.

ABBREVIATIONS: nAChR, nicotinic acetylcholine receptor; ACh, acetylcholine; AChBP, acetylcholine binding protein; DHβE, dihydro-β-erythroidine; ECD, extracellular domain; LBD, ligand binding domain.

attention deficit disorders, and nicotine addiction (Cassels et al., 2005; Taly et al., 2009). The development of new drugs that interact selectively with $\alpha4\beta2$ nAChRs traditionally has focused on agonists (full or partial) and more lately on allosteric potentiators (Arneric et al., 2007). In contrast, drug discovery efforts have paid little attention to $\alpha4\beta2$-selective antagonists. These could be useful pharmacological tools for gaining a better understanding of the physiological processes and diseases involving $\alpha4\beta2$ nAChRs. In addition, there are increasing clinical and preclinical data showing that $\alpha4\beta2$ antagonists are a potential treatment for depression and anxiety (Lippiello et al., 2008).

Erythrina alkaloids constitute a group of natural products isolated mainly from trees and shrubs belonging to the genus *Erythrina*. Of these, erysodine and dihydro-β-erythroidine (DHβE) display high-affinity (low nanomolar K_i values) competitive antagonism for $\alpha4\beta2$ nAChR (Decker et al., 1995; Harvey and Luetje, 1996; Chavez-Noriega et al., 1997; Marks et al., 1999). Erysodine and DHβE also inhibit $\alpha7$ and $\alpha3\beta4$ nAChRs, but with lower affinity (micromolar K_i values) (Decker et al., 1995; Harvey and Luetje, 1996; Chavez-Noriega et al., 1997; Papke et al., 2008). Erysodine is a more potent inhibitor of $\alpha4\beta2$ nAChR than DHβE (Decker et al., 1995), although both alkaloids exhibit similar low affinity for $\alpha7$ nAChR. Thus, although DHβE and erysodine are not subtype-selective, their high affinity for $\alpha4\beta2$ nAChR could be exploited to identify molecular determinants influencing inhibition of this receptor subtype by this class of alkaloids.

Early studies carried out on heterologously expressed nAChRs containing $\alpha3$-$\alpha4$ or $\beta2$-$\beta4$ chimeras or mutant $\alpha3\beta2$ nAChRs (Harvey and Luetje, 1996) identified major determinants of sensitivity to DHβE antagonism that are now recognized to lie within the N-terminal extracellular domain (ECD) of neuronal heteromeric nAChRs. These findings, together with the competitive nature of Erythrina alkaloid inhibition of nAChRs, suggest that inhibition may be at least partly governed by interactions between Erythrina antagonists and the conserved aromatic residues of the agonist binding site of nAChRs. To address this issue, we have taken advantage of the availability of Erythrina alkaloids that are structurally related to DHβE and erysodine (Fig. 1) and homology models of the $\alpha4\beta2$ nAChR (Moroni et al., 2008). By using these in conjunction with mutagenesis and functional assays, we identified the major determinants responsible for sensitivity to inhibition by Erythrina alkaloids. In doing so, we could account for the selectivity of Erythrina alkaloids for $\alpha4\beta2$ nAChR over other nAChR subtypes and provide a plausible molecular mechanism for competitive inhibition of $\alpha4\beta2$ nAChR by Erythrina alkaloids.

Materials and Methods

Chemicals. Erysodine, erysotrine, and erysopine were isolated from seeds of *Erythrina falcata* Benth. Epierythratidine was isolated from seeds of *Erythrina fusca* Lour. All structures were confirmed by using one- and two-dimensional ^{1}H and ^{13}C NMR analyses. The hemisynthetic *O*-acetylerysodine was prepared by direct esterification of erysodine using acetic anhydride in benzene. Purity and structure of the compounds was established by high-resolution one- and two-dimensional NMR experiments and was typically 98 to 100%. DHβE was obtained from Tocris Bioscience (Bristol, UK). Other chemicals were purchased from Sigma Chemical (Poole, Dorset, UK). Fresh ACh stock solutions were made daily in Ringer's solution.

Ligand Binding Assays. Competition binding studies were performed on membrane preparations from the SH-EP1-h$\alpha7$ clonal cell line (Peng et al., 2005), which overexpresses the human $\alpha7$ nAChR, or the SH-EP1-h$\alpha4\beta2$ clonal cell line (Eaton et al., 2003), which expresses human $\alpha4\beta2$ nAChR, using [^{3}H]epibatidine (GE Healthcare, Little Chalfont, Buckinghamshire, UK) or [^{3}H]cytisine (PerkinElmer Life and Analytical Sciences, Cambridge, UK) respectively, as described previously (Houlihan et al., 2001). Membrane homogenates were incubated at a final protein concentration of 30 to 50 μg per assay tube in a final volume of 500 μl ([^{3}H]epibatidine) or 250 μl ([^{3}H]cytisine) of binding saline (120 nM NaCl, 5 nM KCl, 1 nM $MgCl_2$, 2.5 nM $CaCl_2$, and 50 nM Tris, pH 7.0) for 120 min at room temperature (25°C) with 1 nM [^{3}H]epibatidine or for 75 min at 4°C with 1 nM [^{3}H]cytisine. For both binding assays, 10 μM nicotine was used to define nonspecific binding. Bound and free fractions were separated by rapid filtration through Whatman (Clifton, NJ) GF/C filters presoaked in binding saline supplemented with 0.1% polyethylenimine. Radioactivity was quantified by liquid scintillation spectrometry.

Mutagenesis. Site-directed mutagenesis of residues located within the extracellular N-terminal domain of human $\alpha4$ or $\beta2$ subunit cDNAs was performed with a QuikChange kit (Stratagene, Cambridge, UK). The full-length sequence of mutant $\alpha4$ and $\beta2$ subunit cDNAs was verified by DNA sequencing (Geneservice, Oxford, UK). We present the numbering of the amino acid residues in terms of the full length, including the signal sequence. To obtain the position in the mature form, subtract 28 for $\alpha4$ and 26 for $\beta2$.

nAChR Expression in *Xenopus laevis* Oocytes. $\alpha7$ nAChRs or $\alpha4\beta2$ (wild type or mutant) nAChRs were expressed in defolliculated stage V or VI *X. laevis* oocytes, which were dissected from adult female *X. laevis* frogs (European *Xenopus* Resource Centre, Portsmouth University, Portsmouth, UK). The care and use of *X. laevis* frogs in this study was approved by the Oxford Brookes University Animal Research Committee, in accordance with the guidelines of the 1986 Scientific Procedures Act of the United Kingdom. Human $\alpha7$ cDNA or a mixture of $\alpha4$ and $\beta2$ subunit cDNAs at a 1:1 ratio were injected into the nuclei of oocytes in a volume of 18.4 nl/oocyte by using a Nanoject Automatic Oocyte Injector (Drummond Scientific, Broomall, PA). The total amount of cDNA injected per oocyte was kept constant at 2 ng. Note that nuclear injection of equal amounts

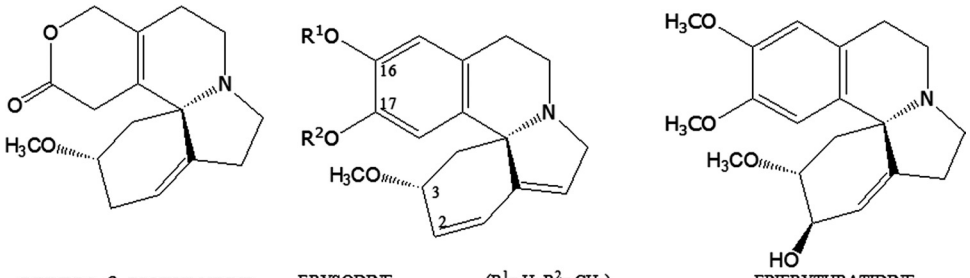

Fig. 1. Left, structure of DHβE. Center, structure of erysodine, erysotrine, erysopine, and *O*-acetylerysodine. Right, structure of epierythratidine.

of $\alpha4$ and $\beta2$ subunits results in a mixture of $\alpha4\beta2$ receptors comprising approximately 20% $(\alpha4)_2(b2)_3$ and 80% $(\alpha4)_3(b2)_2$ nAChR (Moroni et al., 2006). After injection, oocytes were incubated at 19°C in modified Barth's solution containing 88 mM NaCl, 1 mM KCl, 2.4 mM $NaHCO_3$, 0.3 mM $Ca(NO_3)_2$, 0.41 mM $CaCl_2$, 0.82 mM $MgSO_4$, 15 mM HEPES, and 50 μg/ml neomycin (pH adjusted to 7.6 with NaOH). Experiments were performed on oocytes 2 to 6 days after injection.

Electrophysiological Recordings. Oocytes were placed in a 0.1-ml recording chamber and perfused with Ringer's solution (150 mM NaCl, 2.8 mM KCl, 10 mM HEPES, and 1.8 mM $CaCl_2$, pH adjusted to 7.2 with NaOH) at a rate of 15 ml/min. Oocytes were impaled by two agarose-cushioned microelectrodes filled with 3 M KCl (0.3–2.0 MΩ) and voltage-clamped at −60 mV using a GeneClamp 500B amplifier and pCLAMP 8 software (Molecular Devices, Sunnyvale, CA). Typically, traces were filtered at 1 kHz during recording and digitized at 1 kHz by using the DigiData 1200 interface (Molecular Devices). All experiments were carried out at room temperature. Compounds were applied by gravity perfusion using a manually activated valve. ACh concentration-response curves were obtained by normalizing ACh-induced responses to the control responses induced by 1 mM ACh (a near-maximum effective concentration at receptors obtained with 1:1 $\alpha4$ to $\beta2$ cDNA transfecting ratios) (Moroni et al., 2006). A minimum interval of 4 min was allowed between ACh applications because this was found to be sufficient to ensure reproducible recordings. The sensitivity of the receptors to inhibition by antagonists was tested by first superfusing the antagonist for 2 min and then coapplying it with an EC_{50} concentration of ACh (wild-type $\alpha4\beta2$, 100 μM; $\alpha4\beta2$D196A, 100 μM; $\alpha4$W182A$\beta2$, 400 μM; $\alpha4$Y230A$\beta2$, 400 μM; $\alpha4\beta2$W82A, 300 μM; $\alpha4\beta2$T84A, 200 μM; $\alpha7$ nAChR, 100 μM). To assess the effect of mutations on functional expression, the maximal ACh responses of mutant receptors were normalized to the ACh-maximal responses of wild-type $\alpha4\beta2$ expression. Antagonist concentration-response data were normalized to the appropriate ACh EC_{50}. ACh was applied for a period sufficient (approximately 10–15 s) to obtain a stable plateau response (at low concentrations) or the beginning of a sag after a peak (at higher concentrations). Between each successive ACh and/or compound application, the cell was perfused with Ringer's solution for 4 min to allow drug clearance and prevent receptor desensitization. To construct antagonist concentration-effect curves, the responses elicited by coapplication of an EC_{50} ACh concentration and increasing concentrations of compound were normalized to the response elicited by an EC_{50} concentration of ACh alone. ACh EC_{50} concentration at $\alpha4\beta2$ nAChR and $\alpha7$ nAChR was 100 μM (Houlihan et al., 2001; Moroni et al., 2006). Constant responses to ACh were obtained before the coapplication of ACh and compound. In these studies, oocytes were preincubated with compound for 2 min before the coapplication procedure to ensure equilibration between receptors and compounds. To maintain ongoing measurements of the control response to ACh throughout the experiment, each coapplication was bracketed by an application of EC_{50} of ACh alone. To compare accurately the functional expression of mutant and wild-type receptors, the peak amplitude of ACh-induced maximal current responses for mutant receptors was normalized to that for wild-type receptors that were injected on the same day.

Dopamine Release. The measurement of [^{3}H]dopamine release from rat striatal slices was based on a previously described method (Puttfarcken et al., 2000; Livingstone et al., 2009). Rats (250–350 g) were killed by cervical dislocation, and the striata were rapidly dissected. Striatal prisms (0.25 mm) were prepared by using a McIlwain tissue chopper, washed three times with Krebs-bicarbonate buffer (118 mM NaCl, 2.4 mM KCl, 2.4 mM $CaCl_2$, 1.2 mM $MgSO_4$, 1.2 mM KH_2PO_4, 25 mM $NaHCO_3$, and 10 mM glucose, oxygenated with 95% O_2/5% CO_2, pH 7.4), and loaded with 50 nM [^{3}H]dopamine for 30 min at 37°C. After four washes with Krebs buffer plus nomifensine (0.5 μM), slices were dispersed into 96-well multiscreen filter plates (Millipore Corporation, Billerica, MA). Serial dilutions of two compounds were tested in each 96-well plate (half a plate per compound). Striata from two animals were sufficient for one 96-well plate. Buffer was removed by using a vacuum filtration unit (Millipore Corporation), and 70 μl of Krebs buffer containing nomifensine, with or without test compound, was added to each well and allowed to incubate for 5 min at 37°C in an atmosphere of 95% O_2 and 5% CO_2. Basal release was collected via vacuum filtration into a 96-well OptiPlate (PerkinElmer Life and Analytical Sciences) and replaced with 70 μl of buffer (with or without 10 μM nicotine and/or test drug) and incubated for 10 min at 37°C. Stimulated release was collected by vacuum filtration into another 96-well OptiPlate. MicroScint-40 (170 μl; PerkinElmer Life and Analytical Sciences) was added to each well, and radioactivity was counted with a scintillation counter (Wallac MicroBeta TriLux 1450; PerkinElmer). To estimate radioactivity remaining in the slices at the end of the experiment, filters were removed from the 96-well plate and counted for radioactivity. Total radioactivity present in the slices at the start of the stimulation was calculated as the sum of disintegrations per minute tritium released plus disintegrations per minute tritium radioactivity remaining in the slices at the end of the experiment, after correction for counting efficiency. Released radioactivity is presented as a proportion of total radioactivity (fractional release) for each well [stimulated release/(basal release + stimulated release + remaining radioactivity in the tissue) − basal release/(stimulated release + remaining radioactivity)].

Data Analyses. Concentration-effect data for antagonists were fitted by nonlinear regression (Prism 5.0; GraphPad Software Inc., San Diego, CA) to the equation $I = I_{max}/[1 + (IC_{50}/x)^{nH}]$, where I_{max} is maximal normalized current response (in the absence of antagonist for inhibitory currents), x is antagonist concentration, IC_{50} is antagonist concentration eliciting half-maximal inhibition, and n_H is the Hill coefficient. Results are presented as mean ± S.E.M. of at least four separate experiments from at least two different batches of oocytes. The same equation was used to estimate IC_{50} values for inhibition of radioligand binding, and the K_i value of the test compounds was determined by using the equation of Cheng and Prusoff (1973): $K_i = IC_{50}/1 + x/K_D$, where x is the radioligand concentration and K_D is the affinity binding constant.

Statistical significance was assessed by using a two-tailed unpaired t test or one-way analysis of variance followed by the Dunnett post-test as appropriate. $P < 0.05$ is considered significant.

Homology Modeling. The homopentameric acetylcholine binding protein (AChBP) from *Aplysia californica* (Protein Data Bank code 2BYN) (Hansen et al., 2005) was used to generate models of the ECD of the $\alpha4\beta2$ nAChR. This domain houses the agonist binding site of the receptor (Brejc et al., 2001; Hansen et al., 2005). Even though the sequence identity between AChBP and the subunits of the $\alpha4\beta2$ nAChRs is only 18 to 20%, a similar fold and highly conserved binding site residues (Brejc et al., 2001; Hansen et al., 2005) make the AChBP structure suitable for modeling the ECD of nAChRs. Multiple sequence alignment was performed by ClustalW (Thompson et al., 1994), and 200 models of $\alpha4\beta2$ nAChRs were generated by using Modeler 8 (Sali and Blundell, 1993). All generated homology models possessed an explicit disulfide bond between $\alpha4$ residues Cys225 and Cys226 and reproduced the amino acids reported previously as implicated in the binding of agonist by $\alpha4\beta2$ nAChR (Hansen et al., 2005). The best model was energy-minimized in vacuo, using the molecular dynamics package Amber 9 (Case et al., 2006), with 500 cycles of the steepest descent method followed by another 500 cycles of the conjugate gradient method. The quality of the energy-minimized structures was checked with Procheck (http://www.ebi.ac.uk/thornton-srv/software/PROCHECK). Images were generated by using PyMOL (http://www.pymol.org). The overall average g factor for the best structures was −0.20. This value is a good indicator for the quality of the models.

Docking Analysis. Molecular docking of DHβE and Erythrina ligands at the ligand binding domain (LBD) of the $\alpha4\beta2$ homology models was investigated by using the Lamarckian genetic algorithm

search method as implemented in AutoDock version 4.0 (Morris et al., 1998). The receptors were kept rigid, whereas full flexibility was allowed for the ligands to translate/rotate. Polar hydrogens were added to the receptors, and Kollman-united atom partial charges along with atomic solvation parameters were assigned to the individual protein atoms. The three-dimensional structures of each ligand were generated by using the GaussView program (http://www-.gaussian.com). Ligands were then energy-minimized by using Gaussian98 software. For each ligand, a rigid root and rotatable bonds were assigned automatically. The nonpolar hydrogens were removed, and the partial charges from these were added to the carbon (Gasteiger charges). The atom type for aromatic carbons was reassigned to use the AutoDock 4.0 aromatic carbon grid map. Docking was carried out by using $60 \times 60 \times 60$ grid points with a default spacing of 0.375 Å. The grid was positioned to include the full ligand binding pocket in the central part of the $\alpha4/\beta2$ subunit interfaces to allow extensive sampling around residue $\alpha4$Trp182 (Trp143 in mature AChBP). Within this grid, the Lamarckian genetic search algorithm was used with a population size of 150 individuals, calculated by using 200 different runs (i.e., 200 dockings). Each run had two stop criteria, a maximum of 1.5×10^6 energy evaluations or a maximum of 50,000 generations, starting from a random position and conformation; default parameters were used for the Lamarckian genetic algorithm search.

Results

Interactions of Erythrina Alkaloids with $\alpha4\beta2$ nAChRs. The effects of the Erythrina alkaloids DHβE, erysodine, erysotrine, erysopine, *O*-acetylerysodine, and epierythratidine (Fig. 1) on the binding of [^{3}H]cytisine to $\alpha4\beta2$ nAChRs were examined by using membrane homogenates prepared from SH-EP1-h$\alpha4\beta2$ clonal cells. The skeleton for all of these alkaloids, including that of DHβE that has a lactone group in lieu of an aromatic ring, consists of a tetracyclic spiroamine system comprising a protonated nitrogen atom and substituents at positions C-2, C-3, C-15, and C-16. Figure 2A shows that specific binding of [^{3}H]cytisine to $\alpha4\beta2$ nAChR was fully displaced by all six Erythrina alkaloids in a concentration-dependent manner. Estimated K_i values are summarized in Table 1. Erysodine, which has a hydroxyl group at position 16 and a methoxyl group at position 15, was the most potent of these compounds (K_i 50 nM), whereas the least potent compound was epierythratidine (K_i 710 nM), an alkaloid with methoxyl groups at positions 15 and 16 and at position 3 and an additional hydroxyl at position 2. Erysopine, which differs from erysodine in that there are hydroxyl groups at both Cys15 and Cys16, displayed moderate potency (K_i 154 nM). Erysotrine, which is identical to epierythratidine except that it lacks a hydroxyl group at position 2, was markedly less potent than erysopine (K_i 604 nM) but more potent than epierythratidine (K_i 710 nM). The K_i values for DHβE (98 nM), and *O*-acetylerysodine (K_i 79 nM), which has an acetyl carbonyl group at position 16 and a methoxyl group at position 15, were not significantly different from each other; these compounds were less potent than erysodine but more potent than all of the other alkaloids tested. Summarizing, the rank order of potency for displacement of [^{3}H]cytisine from $\alpha4\beta2$ nAChRs by Erythrina alkaloids is: erysodine $>$ *O*-acetylerysodine $\approx$ DHβE $>$ erysopine $>$ erysotrine $>$ epierythratidine.

All six Erythrina alkaloids inhibited the function of $\alpha4\beta2$ nAChRs expressed heterologously in *X. laevis* oocytes (Fig. 2, B and C). Inhibition of ACh-evoked currents was concentration-dependent, and the estimated IC_{50} values ranged from 96 nM (erysodine) to 4923 nM (epierythratidine) (data listed in Table 2). The rank order of potency for functional inhibition of $\alpha4\beta2$ nAChR mirrored that found for the inhibition of [^{3}H]cytisine binding, except that the potencies of DHβE, erysodine, and *O*-acetylerysodine were not statistically different from each other. The similarity between the rank order of

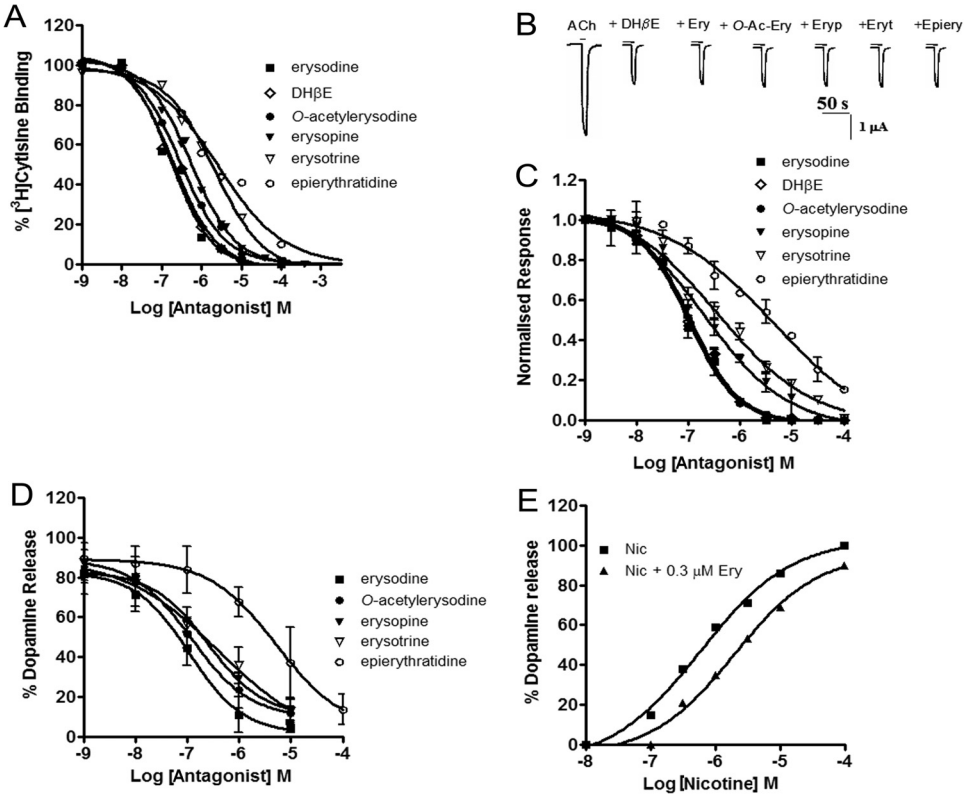

Fig. 2. Effects of Erythrina alkaloids on the function and radioligand binding to human $\alpha4\beta2$ nAChRs. A, displacement of [^{3}H]cytisine binding to SH-EP-h$\alpha4\beta2$ by Erythrina alkaloids. SH-EP1-h$\alpha4\beta2$ membrane homogenates were incubated with 1 nM [^{3}H]cytisine for 75 min at 4°C in the presence of various concentrations of Erythrina alkaloids. B, traces showing responses of oocytes expressing $\alpha4\beta2$ nAChRs to the application of 100 μM ACh alone or coapplied with IC_{50} concentrations of either DHβE, erysodine (Ery), *O*-acetylerysodine (*O*-Ac-Ery), erysopine (Eryp), erysotrine (Eryt), or epierythratidine (Epiery). Erythrina alkaloids were coperfused with 100 μM ACh (EC_{50}) after 2 min of exposure to alkaloid alone. C, concentration-response curves for inhibition by Erythrina alkaloids of ACh-evoked currents in oocytes expressing $\alpha4\beta2$ nAChRs. Data points represent the mean ± S.E.M. of at least three experiments. D, inhibition of nicotine-evoked [^{3}H]dopamine release from rat striatal slices by Erythrina alkaloids. E, competitive inhibition of 300 nM erysodine on the concentration-response curve for nicotine-evoked release of [^{3}H]dopamine. Each point represents the mean ± S.E.M. of at least three separate experiments, each conducted with eight replicates.

potency of inhibition of $\alpha4\beta2$ nAChR function and binding of [^{3}H]cytisine to $\alpha4\beta2$ suggests that the structural determinants that affect the binding of the alkaloids to $\alpha4\beta2$ nAChRs also influence their functional effects, as expected for competitive antagonists.

To test whether the above Erythrina alkaloids inhibit native $\alpha4\beta2$ nAChRs with the same rank order of potency that they inhibit recombinant $\alpha4\beta2$ nAChRs, the alkaloids were compared for their abilities to inhibit nicotine-evoked [^{3}H]dopamine release from rat striatal slices. All of the alkaloids tested inhibited [^{3}H]dopamine release fully and with potencies that closely matched those estimated from the electrophysiological measurements on recombinant $\alpha4\beta2$ nAChRs, to give a comparable rank order of potency of inhibition (Fig. 2D; IC_{50} values listed in Table 2). Competitive antagonism was demonstrated for nicotine-evoked [^{3}H]dopamine release by erysodine (Fig. 2E).

Effects of Erythrina Alkaloids on $\alpha7$ nAChR. Previous studies using native and recombinant nAChR have shown erysodine and DHβE to have high selectivity for $\alpha4\beta2$ nAChR over $\alpha7$ nAChR (Decker et al., 1995; Chavez-Noriega et al., 1997). To determine whether this distinction applies to all of the Erythrina alkaloids studied here in relation to $\alpha4\beta2$ nAChRs, we conducted both [^{3}H]epibatidine binding displacement assays and concentration-functional inhibition studies of recombinant $\alpha7$ nAChR for all of these alkaloids. As shown in Fig. 3, all Erythrina alkaloids examined were poor inhibitors of [^{3}H]epibatidine binding to $\alpha7$ nAChRs (Fig. 3A; data summarized in Table 1), with K_i values ranging from 7500 nM (erysodine) to 14,670 nM (erysopine). These antagonists were capable of inhibiting the function of $\alpha7$ nAChRs, but the estimated IC_{50} values were on the average 3 orders of magnitude higher than those for inhibition of $\alpha4\beta2$ nAChR function (Fig. 3B; IC_{50} values listed in Table 2). It is noteworthy that the Erythrina inhibitors seemed to slow down the decay of the responses to ACh (Fig. 3B), suggesting that they may induce changes in current kinetics. In addition, we noticed that the concentration-response curves for the inhibition of $\alpha7$ nAChRs by Erythrina alkaloids do not plateau at zero. This, together with the changes in current kinetics, suggests that the Erythrina alkaloids may also act through a noncompetitive mechanism. Further characterization is necessary to identify the mechanism of noncompetitive inhibition and understand the extent of competitive and noncompetitive blockade. Although Erythrina alkaloids were significantly less potent at inhibiting $\alpha7$ nAChR, the rank order of potency for inhibition of this receptor type was similar to that for the inhibition of $\alpha4\beta2$ nAChRs.

Mutation of Conserved Aromatic Residues in $\alpha4$ and $\beta2$ Subunits. So far, the above studies have shown that of all the Erythrina alkaloids tested erysodine and DHβE are the most potent inhibitors of $\alpha4\beta2$ nAChRs. We therefore chose these two antagonists for studies aimed at elucidating molecular determinants for the inhibition of $\alpha4\beta2$ nAChRs by Erythrina alkaloids. Because of previous findings showing that competitive inhibitors interact with the agonist binding site of the AChBP (Hansen et al., 2005) and the ECD of both neuronal α and β nAChR subunits contribute determinants for DHβE sensitivity (Harvey and Luetje, 1996), we focused these studies on the conserved aromatic residues of the agonist binding site of the nAChR (Brejc et al., 2001; Unwin, 2005; Taly et al., 2009). In the $\alpha4\beta2$ nAChR these residues are α4Tyr126, α4Trp182, α4Tyr223, α4Tyr230, and β2Trp82. For comparison, the corresponding homologous residues in mature *Torpedo* nAChR are α1Tyr93, α1Trp149, α1Tyr190, α1Tyr198, and γTrp55 (Unwin, 2005). To elucidate which of these residues contribute to the sensitivity to erysodine or DHβE, we mutated each residue separately to create α4Y126A, α4W182A, α4Y223A, α4Y230A, and β2W82A single mutants. In addition, we mutated the nonconserved residue β2Thr84 to alanine because this residue was identified previously as a major determinant of sensitivity to inhibition by DHβE (Har-

TABLE 1

Effects of Erythrina alkaloids on [^{3}H]cytisine binding to α4b2 nAChR and [^{3}H]epibatidine binding to $\alpha7$ nAChR

Data represent the mean ± S.E.M. of three to four experiments. For both [^{3}H]cytisine and [^{3}H]epibatidine bindings, the radiolabeled ligand concentration was 1 nM. K_i values were calculated by using the Cheng and Prusoff (2003) equation, $K_i = IC_{50}/1 + x/K_D$. The K_D value for [^{3}H]cytisine binding was 0.4 nM (Houlihan et al., 2001) and for [^{3}H]epibatidine binding it was 1 nM.

Compound	K_i	
	[^{3}H]Cytisine Binding to $\alpha4\beta2$ nAChR	[^{3}H]Epibatidine Binding to $\alpha7$ nAChR
	nM	
DHβE	98 ± 6	10,500 ± 400
Erysodine	50 ± 3**	7500 ± 150**
O-Acetylerysodine	79 ± 8	7340 ± 230**
Erysopine	154 ± 6**	14,670 ± 1000*
Erysotrine	604 ± 5***	N.E.
Epierythratidine	710 ± 9***	N.E.

N.E., no effects at the highest concentration of inhibitor tested, 1 mM.
*, $P < 0.05$; **, $P < 0.01$; ***, $P < 0.001$, relative to the effects of DHβE.

TABLE 2

Functional effects of Erythrina alkaloids on the function of recombinant and native nAChRs

Data represent the mean ± S.E.M. of three to four experiments. $\alpha7$ and $\alpha4\beta2$ nAChRs were expressed heterologously in *X. laevis* oocytes as described under *Materials and Methods*. The effect of Erythrina alkaloids on the function of native a4$\beta2$* nAChRs was determined by measuring the effects of the inhibitors on nicotine-evoked [^{3}H]dopamine release from rat striatal slices.

Compound	IC_{50}		
	nAChR		Nicotine-Mediated [^{3}H]Dopamine Release
	$\alpha4\beta2$	$\alpha7$	
	nM		
DHβE	110 ± 11	10,101 ± 1870	N.D.
Erysodine	96 ± 25	9532 ± 2000	108 ± 11
O-Acetylerysodine	105 ± 43	14,543 ± 5400	120 ± 16
Erysopine	201 ± 20*	16,676 ± 6000*	250 ± 20**
Erysotrine	367 ± 16***	16,987 ± 3000*	402 ± 33***
Epierythratidine	4923 ± 150***	N.E.	5400 ± 40***

N.D., not determined; N.E., no functional effects at the highest concentration of inhibitor tested, 1 mM.
*, $P < 0.05$; **, $P < 0.01$; and ***, $P < 0.001$ in comparison with the effects of DHβE (recombinant a4$\beta2$ nAChR) or erysodine (dopamine release).

vey and Luetje, 1996). For all mutants of the conserved aromatic residues (except for α4Y223A that reduced function below the limits of detection; Table 3), we found that functional sensitivity to ACh was reduced significantly (Table 3). In addition, all mutations, except α4W182A, caused a significant decrease in relative ACh maximal responses (Table 3). Overall, the findings so far are in general accord with previously reported mutagenesis studies of α7 (Galzi et al., 1991; Horenstein et al., 2007; Williams et al., 2009) and α4β2 (Horenstein et al., 2007; Williams et al., 2009), further supporting a role for these residues in receptor activation. The concentration-response effects of DHβE and erysodine on the current responses of the mutant receptors to EC_{50} concentrations of ACh (wild-type α4β2, 100 μM; α4β2D196A, 100 μM; α4W182Aβ2, 400 μM; α4Y230Aβ2, 400 μM; α4β2W82A, 300 μM; α4β2T84A, 200 μM) are shown in Fig. 4, A and B, and the estimated IC_{50} values are listed in Table 3. Introducing α4W182A, α4Y126A, α4Y230A, or β2W82A into α4β2 nAChRs decreased sensitivity to inhibition by either erysodine or DHβE. Of all of these mutations, α4Y126A had the most pronounced impact on sensitivity to inhibition (200-fold decrease in comparison to 50-fold for α4W182A, 30-fold for α4Y230A, and 13-fold for β2W82A). Finally, in accord with the findings of Harvey and Luetje (1996), incorporating β2T84A in α4β2 receptors reduced sensitivity to inhibition, although in comparison with β2W82A the decrease was very modest (1.6-fold). These studies show that α4Tyr126, α4Trp182, α4Tyr223, α4Tyr230, β2Trp82, and β2Thr84 contribute to sensitivity to competitive inhibition by DHβE or erysodine.

Homology Modeling of the a4β2 nAChR Binding Domain with Erythrina Alkaloids. To gain insight into how Erythrina alkaloids may interact with α4β2 nAChR to inhibit

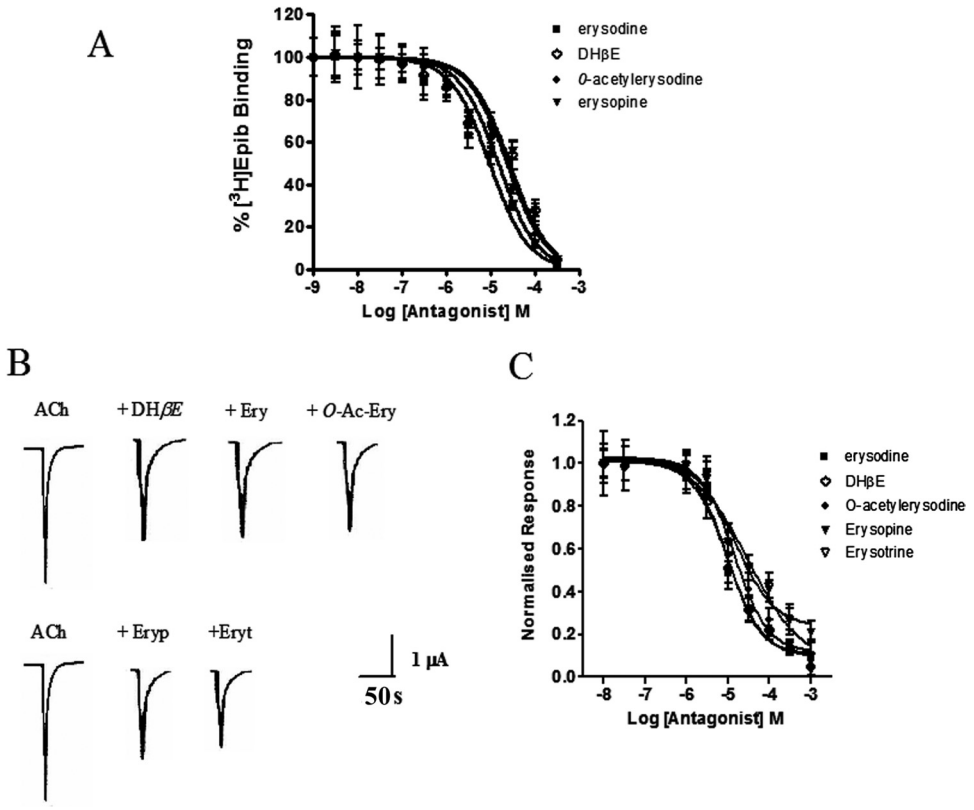

Fig. 3. Effects of Erythrina alkaloids on the function and radioligand binding to human α7 nAChRs. A, displacement of [^{3}H]epibatidine (Epi) binding to SH-EP-hα7 by Erythrina alkaloids. SH-EP1-hα7 membrane homogenates were incubated with 1 nM [^{3}H]epibatidine for 120 min at room temperature in the presence of various concentrations of Erythrina alkaloids. B, responses of oocytes expressing α7 nAChRs to the application of 100 μM ACh alone or coapplied with IC_{50} concentrations of either DHβE, erysodine (Ery), *O*-acetylerysodine (*O*-Ac-Ery), erysopine (Eryp), or erysotrine (Eryt). C, concentration-response curves for inhibition of α7 nAChRs by Erythrina alkaloids. Data points represent the mean ± S.E.M of three to four experiments.

TABLE 3

Functional effects of ACh, DHβE, and erysodine on wild-type and N-terminal domain mutant α4β2 nAChRs

Data represent the mean ± S.E.M. of *n* number of experiments. Wild-type and mutant α4β2 nAChRs were expressed heterologously in *X. laevis* oocytes as described under *Materials and Methods*.

	ACh		IC_{50}		*n*
	I/Wild-type I_{max}	EC_{50}	DHβE	Erysodine	
		μM	μM	μM	
α4β2	1	92 ± 21	0.11 ± 0.009	0.096 ± 0.005	10
α4Y126Aβ2	0.22 ± 0.1**	530 ± 100*	20 ± 12**	19 ± 8**	3
α4W182Aβ2	0.87 ± 0.06	451 ± 54**	5.5 ± 0.5***	4.43 ± 0.11**	7
α4Y223Aβ2	N.A.	N.A.	N.A.	N.A.	4
α4Y230Aβ2	0.25 ± 0.08**	401 ± 45**	3.2 ± 0.4***	3.17 ± 0.9**	6
α4β2D196A	0.98 ± 0.1	114 ± 45	N.E.	N.E.	10
α4β2W82A	0.42 ± 0.09*	313 ± 61*	1.41 ± 0.8**	2 ± 0.8**	6
α4β2T84A	0.51 ± 0.09*	201 ± 28*	0.87 ± 0.1***	1.2 ± 0.4**	6

N.A., not available (current responses were below the limits of detection); N.E., no functional effects at the highest concentration of inhibitor tested, 1 mM.
*, $P \leq 0.05$; **, $P < 0.01$; ***, $P < 0.001$, relative to effects on wild-type α4β2 receptors.

receptor activation, the alkaloids were docked in the ECD of the $\alpha4\beta2$ nAChR based on homology modeling. The lactone group of DHβE and the aromatic ring of erysodine, erysopine, erysotrine, *O*-acetylerysodine, and epierythratidine (Fig. 5) lay clearly inside the aromatic cage formed by $\alpha4$ residues Tyr126, Tyr223, Tyr230, and Trp182, with the lactone moiety of DHβE or the hydroxyl substituent at C-16 in erysodine and erysopine or the acetyl carbonyl group in *O*-acetylerysodine positioned within hydrogen bond distance to $\alpha4$Tyr126. This prediction correlates well with the findings of our mutagenesis studies showing that $\alpha4$Y126A$\beta2$ nAChRs are less sensitive to inhibition by erysodine or DHβE than their wild-type counterpart. $\alpha4$Tyr126 seemed to act as a hydrogen-bonding acceptor or donor depending on whether the bonding partner was erysodine, erysopine, DHβE, or *O*-acetylerysodine. In contrast, the methoxyl group at C-16 in erysotrine or epierythratidine, both of which display low inhibitory potency at $\alpha4\beta2$ nAChRs, docked away from $\alpha4$Tyr126 (Fig. 5D). The methoxyl group at C-16 in the latter alkaloids seems to have a repulsive interaction with the receptor surface, pushing the ligand away from it. Consistent with these observations, the $\alpha4$Y126A mutation had little effect on the inhibition of ACh-evoked currents by erysotrine or epierythratidine compared with wild-type $\alpha4\beta2$ receptors (erysotrine: IC_{50} $\alpha4\beta2 = 367 \pm 16$ μM; IC_{50} $\alpha4$Y126A = 401 ± 68 μM; $n = 3$; epierythratidine: IC_{50} $\alpha4\beta2 = 4923 \pm 150$ μM; IC_{50} $\alpha4$Y126A$\beta2 = 5025 \pm 345$ μM; $n = 4$) (not shown).

None of the alkaloids examined seem to engage in cation-π interactions between the protonated nitrogen and $\alpha4$Trp182. Instead, the tetrahydroisoquinoline moiety of all six alkaloids seemed to establish van der Waals contacts with the indole ring of $\alpha4$Trp182. The substituent at position C-15 oriented toward loop C, although $\alpha4$Tyr223 and $\alpha4$Tyr230 were not predicted to contact the docked Erythrina alkaloids. This observation is at odds with the finding that Y230A decreased sensitivity to inhibition. Likewise, $\beta2$Trp82 or $\beta2$Thr84, both of which when substituted by alanine decreased sensitivity to inhibition, did not seem to make direct contact with bound Erythrina alkaloids.

Models for all the Erythrina alkaloids except epierythratidine showed unexpectedly that $\beta2$Asp196, a residue located near the entrance of the binding site opposite to loop C, made the most salient contact with the protonated nitrogen present in these ligands, at a distance of approximately 1.7 Å for erysodine, *O*-acetylerysodine, erysopine, and erysotrine and 2.1 Å for DHβE (Figs. 5 and 6B). In the case of epierythratidine, the protonated nitrogen lay 6.2 Å away from $\beta2$Asp196, suggesting that an interaction between these two centers may have little relevance to sensitivity to inhibition by epierythratidine. A comparison between the homology models of unbound $\alpha4\beta2$ and erysodine-bound $\alpha4\beta2$ revealed that in the latter loop C acquired an extended conformation (Fig. 6B), consistent with findings that bound antagonists uncap loop C in the AChBP (Hansen et al., 2005).

$\beta2$Asp196 Is a Key Determinant of Sensitivity to Inhibition by DHβE and Erysodine. The studies described above suggested that $\beta2$Asp196 within the $\alpha4\beta2$ LBD may be a major contributor to sensitivity of $\alpha4\beta2$ nAChRs to inhibition by Erythrina alkaloids. We examined this proposal on human $\alpha4\beta2$ nAChRs by mutating $\beta2$Asp196 to alanine. Introducing $\beta2$D196A completely disrupted the ability of both DHβE and erysodine to inhibit the function of $\alpha4\beta2$ nAChRs. Figure 4 shows that erysodine and DHβE did not inhibit the function of $\alpha4\beta2$ nAChR when applied at the highest concentration tested (300 μM). In contrast, the functional sensitivity of $\alpha4\beta2$D196A to ACh was indistinguishable ($EC_{50} = 96 \pm 12$ μM) from that of the wild-type $\alpha4\beta2$ nAChR ($EC_{50} = 100 \pm 9$ μM), suggesting that the mutation selectively affected Erythrina alkaloid-mediated inhibition and did not induce a general perturbation on $\alpha4\beta2$ function. These studies support the prediction that $\beta2$Asp196 contributes to Erythrina alkaloid binding, forming part of an Erythrina alkaloid inhibitory site predicted to reside at the binding site of $\alpha4\beta2$ nAChR. To further test this prediction we challenged $\alpha4\beta2$Asp196A nAChR with increasing concentrations of epierythratidine, which is not expected to establish strong ionic bonds with $\beta2$Asp196, and found no significant changes in the sensitivity to inhibition of these receptors relative to that of their wild-type counterparts. The estimated epierythratidine IC_{50} value for $\alpha4\beta2$D196A nAChR was 5150 ± 270 nM, and for wild-type $\alpha4\beta2$ nAChR it was 4923 ± 150 nM ($n = 3$) (not shown).

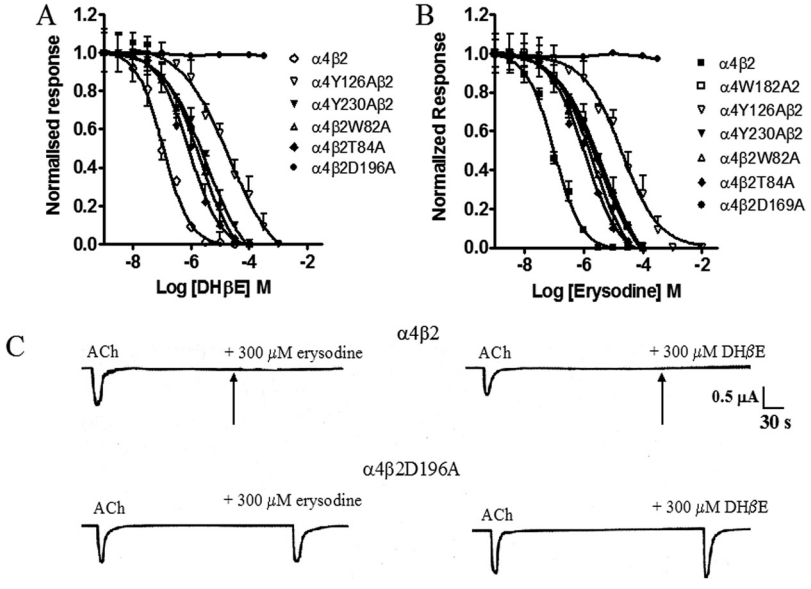

Fig. 4. Inhibition of wild-type and mutant human $\alpha4\beta2$ nAChR by DHβE or erysodine. A and B, the effect of replacement of LBD residues with alanine on sensitivity to inhibition by DHβE (A) or erysodine (B) was investigated by obtaining full concentration-response relationships and estimation of the IC_{50} for each of the Erythrina alkaloids investigated. Data points represent the mean ± S.E.M of 3 to 10 experiments. C, traces showing the pivotal effect of $\beta2$Asp196 on the sensitivity to inhibition of $\alpha4\beta2$ nAChR by DHβE or eysodine. Substitution of $\beta2$Asp196 with alanine completely abolished sensitivity to inhibition by DHβE or erysodine.

Discussion

This study reports the identification of the Erythrina alkaloid binding site on the α4β2 nAChR and a possible molecular mechanism for Erythrina alkaloid-mediated competitive inhibition involving uncapping of loop C in accord with current views on antagonist-induced reorganization of the agonist binding site of Cys loop receptors (Hansen et al., 2005). The conserved aromatic residues within loops A (Tyr126) and B (Trp182) of the α4 subunit and a moderately conserved aspartate residue within β2 (Asp196) are predicted to interact with Erythrina alkaloids, and they all influence the sensitivity of α4β2 nAChR to inhibition by these compounds. When this ability was abolished, through alanine substitution, the sensitivity to inhibition was either decreased (as for α4Y126A and α4Trp182) or completely eliminated (as for β2Asp196). In addition, residues within loop C in the α4 subunit or loop D in the β2 subunit, which are not predicted to contact receptor bound Erythrina alkaloids, decreased sensitivity to inhibition, when substituted with alanine. These residues may contribute allosterically to the signal transduction from the Erythrina alkaloid binding site. Alternatively, the effects of the alanine mutants of these residues on inhibition may merely reflect a general impairment in receptor function.

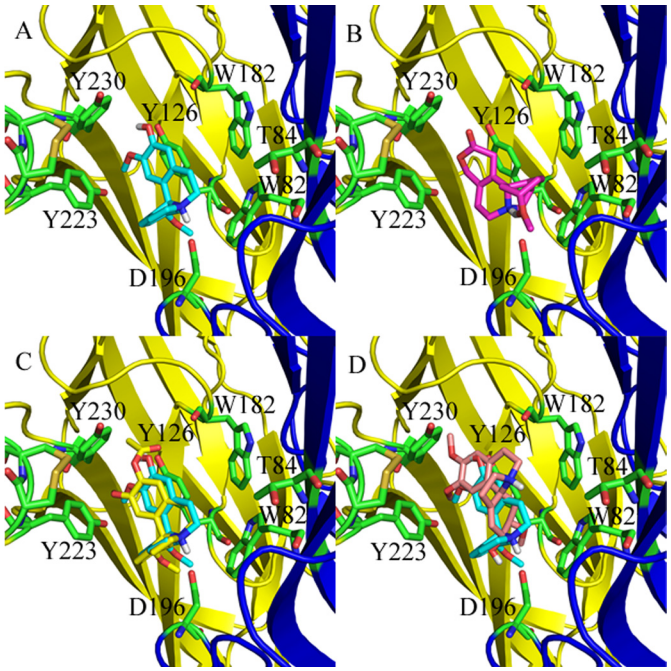

Fig. 5. Predicted docking of tetracyclic Erythrina alkaloids into α4β2 nAChR homology models. A and B, erysodine (light blue) (A) and DHβE (magenta) (B). C and D, for comparison, *O*-acetylerysodine (yellow) (C) and epierythratidine (pink) (D) are shown against the background of bound erysodine (light blue).

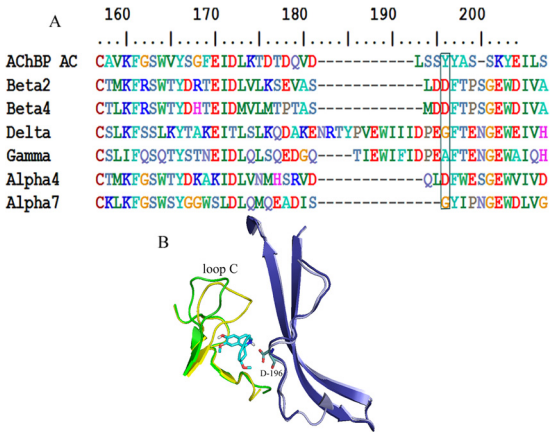

Fig. 6. A, alignment showing that β2Asp196 is weakly conserved in nAChR. B, comparison of the conformation of loop C in agonist-unbound and antagonist-bound conditions.

α4Tyr126 is predicted to hydrogen-bond with the hydroxyl group at C-16 in erysodine and erysopine, the lactone group in DHβE, and the acetyl carbonyl group at C-16 in *O*-acetylerysodine, and this interaction is likely to contribute to sensitivity to inhibition by these antagonists. Consistent with this view, substitution of Tyr126 with alanine significantly impaired the ability of both erysodine and DHβE to inhibit the function of α4β2 nAChRs. That this interaction may critically underlie sensitivity to inhibition is supported further by the finding that both Erythrina alkaloids lacking a hydroxyl substituent at C-16 (e.g., erysotrine and epierythratidine) were weak inhibitors of α4β2 nAChR and that this limited capability was not impaired by α4Y126A. The case of *O*-acetylerysodine is interesting in that the acetyl carbonyl group can form a hydrogen bond with α4Tyr126, with its methyl group fitting into a fairly deep pocket in the receptor. This result could explain the similar affinity and potency of *O*-acetylerysodine and erysodine. Thus, a tentative structure-activity relationship for the aromatic Erythrina alkaloids is that a hydrogen-bonding substituent at C-16 favors interactions with α4Tyr126 and hence high affinity for the α4β2 nAChR.

The conserved α4Trp182 residue binds ACh via strong cation-π interactions (Zhong et al., 1998; Beene et al., 2002), which makes the protonated nitrogen atom of nonquaternary agonists a key pharmacophore (Tønder and Olesen, 2001). Erythrina alkaloids are also endowed with a protonated nitrogen but this is not predicted to establish cation-π interactions with α4Trp182. Instead, our homology models of the antagonist-bound α4β2 nAChR suggest the much weaker van der Waals type of contacts between these compounds and the aromatic indole ring of α4Trp182. This prediction is consistent with the observation that α4W182A reduced sensitivity to inhibition by erysodine or DHβE to a lesser extent that α4Y126A or β2D196A. A possible structural reason for this is that the ammonium center in typical agonists is exposed to the receptor surface, whereas in the Erythrina alkaloids this atom is part of a more sterically demanding cage structure and is thus less accessible to the bulky α4Trp182 π system. Consequently, Erythrina alkaloids orient their nitrogen atom toward a more accessible β2Asp196 with which they establish strong ionic bonds.

Substitution of β2Trp82 or β2Thr84 with alanine decreased sensitivity to inhibition, yet neither of these residues are predicted to interact with Erythrina alkaloids. These residues could contribute allosterically to the downstream signal transduction from the inhibitor binding site. The highly conserved β2Trp82 and the weakly conserved β2Thr84 are located within loop D in the β2 subunit from which they could affect the inhibitory signal generated upon binding of the antagonist to the receptor. Loop D is positioned between α4Trp182 and α4Tyr126, facing the plus interface of the agonist binding site (Brejc et al., 2001; Hansen et al., 2005), and its conformation

could potentially be affected by the contacts between Erythrina antagonists and α4Trp182 and α4Tyr126, which in turn could either affect interior intrasubunit interactions associated with receptor inhibition. This view is supported by structural data from the AChBP that suggest that structural reorganization of the ECD associated with receptor activation or inactivation may be ligand-specific (Hansen et al., 2005). An alternative possibility is that these residues affect sensitivity to inhibition purely because of the contribution of loop D to receptor function (Brejc et al., 2001; Hansen et al., 2005; Bafna et al., 2009; Williams et al., 2009), a view that is consistent with the finding that substitution of these residues by alanine impaired sensitivity to activation by ACh.

As for β2Trp82 or β2Thr84, substitution of α4Tyr230 for alanine brought about a decrease in sensitivity to inhibition, even though this residue is not predicted to contact bound Erythrina antagonists. What may be the role of loop C in Erythrina alkaloid-mediated inhibition of α4β2 nAChRs? The relationship between loop C and sensitivity to inhibition by β2Asp196 suggest loop C as an allosteric contributor to the inhibitory signal generated by the bound antagonist, although a general perturbation on α4β2 receptor function brought about by the incorporation of α4Y230A cannot be discarded. From our homology models of antagonist-bound α4β2 nAChR we cannot predict the type of contacts that may occur between β2Asp196 and loop C or between loop C and the ECD loops with which β2Asp196 seems to interact. It may be that the interactions predicted for the antagonist and residues α4Tyr126, α4Trp182, and β2Asp196 trigger a concerted reorganization of the agonist binding domain, including uncapping of loop C. In this scenario, a change in the structure of loop C brought about by α4Y230A would affect sensitivity to inhibition, even in the absence of contacts between residue Tyr230 and the antagonist. In support of this view, recent structure-functional studies in nAChR have revealed that loop B contacts loops A and C on the principal binding face (Grutter et al., 2003; Mukhtasimova et al., 2005).

β2Asp196 is the major contributor to the sensitivity of α4β2 nAChR to inhibition by Erythrina alkaloids. First, in comparison to the conserved aromatic residues within the agonist binding site of α4β2 nAChR, substitution of β2Asp196 with alanine abolished sensitivity to inhibition by erysodine and DHβE. Second, our homology models of antagonist-bound α4β2 nAChR predict strong ionic bonds between β2Asp196 and the ammonium center of the Erythrina alkaloid inhibitors, and the ability of the Erythrina alkaloids to establish this type of interaction with β2Asp196 correlates well with their potency. Thus, epierythratidine that is not predicted to form ionic bonds with β2Asp196 was the weakest inhibitor of α4β2 nAChR tested, and its potency was not diminished by mutant β2D196A. In addition, β2Asp196 confers receptor subtype selectivity. This residue is weakly conserved within the nAChR family (Fig. 6A), and its absence correlates with low sensitivity to inhibition. For example, the residue is not conserved by α7, γ, or ε subunits, and these subunits form receptors that are inhibited by DHβE or erysodine with micromolar K_i affinities.

How could ionic bonding between β2Asp196 and Erythrina alkaloids lead to receptor inhibition? β2Asp196 is predicted to lie in close proximity to loop C, which upon antagonist binding acquires an extended conformation away from the aromatic nest of the agonist binding site (Fig. 6B). This structural reorganization is consistent with structures of agonist- or antagonist-bound AChBP showing that a closed (capped) loop C is preferred for the active conformation of nAChRs, whereas an open or extended (uncapped) loop C is associated with antagonist-bound (Hansen et al., 2005) or inactive AChBP (Mukhtasimova et al., 2009). Furthermore, the importance of loop C for receptor inhibition was also highlighted by the effect of α4Tyr230 on sensitivity to inhibition by the alkaloids. Thus, our findings indicate that β2Asp196 is the principal residue that confers antagonist activity and receptor subtype selectivity for Erythrina alkaloids and will be an important influence on the preference for open and closed states of the loop C. We feel that these observations could be a useful basis for the design of new, surmountable, high-affinity nAChR antagonists.

Acknowledgments

We thank Ruud Zwart (Eli Lilly, Surrey, UK) and Mirko Moroni (Department of Pharmacology, University College London, London, UK) for critical reading of this manuscript and preparation of figures.

References

Arneric SP, Holladay M, and Williams M (2007) Neuronal nicotinic receptors: a perspective on two decades of drug discovery research. *Biochem Pharmacol* **74:** 1092–1101.

Bafna PA, Jha A, and Auerbach A (2009) Aromatic residues εTrp-55 and δTrp-57 and the activation of acetylcholine receptor channels. *J Biol Chem* **284:**8582–8588.

Beene DL, Brandt GS, Zhong W, Zacharias NM, Lester HA, and Dougherty DA (2002) Cation-π interactions in ligand recognition by serotonergic (5-HT3A) and nicotinic acetylcholine receptors: the anomalous binding properties of nicotine. *Biochemistry* **41:**10262–10269.

Brejc K, van Dijk WJ, Klaassen RV, Schuurmans M, van Der Oost J, Smit AB, and Sixma TK (2001) Crystal structure of an ACh-binding protein reveals the ligand-binding domain of nicotinic receptors. *Nature* **411:**269–276.

Case DA, Darden TA, Cheatham TE III, Simmerling CL, Wang J, Duke RE, Luo R, Merz KM, Pearlman DA, Crowley M, et al. (2006) *AMBER 9*, University of California, San Francisco.

Cassels BK, Bermúdez I, Dajas F, Abin-Carriquiry JA, and Wonnacott S (2005) From ligand design to therapeutic efficacy: the challenge for nicotinic receptor research. *Drug Discovery Today* **10:**1657–1665.

Chavez-Noriega LE, Crona JH, Washburn MS, Urrutia A, Elliott KJ, and Johnson EC (1997) Pharmacological characterization of recombinant human neuronal nicotinic acetylcholine receptors hα2β2, hα2β4, hα3β2, hα3β4, hα4β2, hα4β4 and hα7 expressed in *Xenopus* oocytes. *J Pharmacol Exp Ther* **280:**346–356.

Cheng Y and Prusoff WH (1973) Relationship between the inhibition constant (K1) and the concentration of inhibitor which causes 50 per cent inhibition (I50) of an enzymatic reaction. *Biochem Pharmacol* **22:**3099–3108.

Decker MW, Anderson DJ, Brioni JD, Donnelly-Roberts DL, Kang CH, O'Neill AB, Piattoni-Kaplan M, Swanson S, and Sullivan JP. J (1995) Erysodine, a competitive antagonist at neuronal nicotinic acetylcholine receptors. *Eur J Pharmacol* **280:** 79–89.

Eaton JB, Peng JH, Schroeder KM, George AA, Fryer JD, Krishnan C, Buhlman L, Kuo YP, Steinlein O, and Lukas RJ (2003) Characterization of human α4β2-nicotinic acetylcholine receptors stably and heterologously expressed in native nicotinic receptor-null SH-EP1 human epithelial cells. *Mol Pharmacol* **64:**1283–1294.

Galzi JL, Bertrand D, Devillers-Thiéry A, Revah F, Bertrand S, and Changeux JP (1991) Functional significance of aromatic amino acids from three peptide loops of the α7 neuronal nicotinic receptor site investigated by site-directed mutagenesis. *FEBS Lett* **294:**198–202.

Grutter T, Prado de Carvalho L, Le Novère N, Corringer PJ, Edelstein S, and Changeux JP (2003) An H-bond between two residues from different loops of the acetylcholine binding site contributes to the activation mechanism in nicotinic receptors. *EMBO J* **22:**1990–2003.

Hansen SB, Sulzenbacher G, Huxford T, Marchot P, Taylor P, and Bourne Y (2005) Structures of *Aplysia* AChBP complexes with nicotinic agonists and antagonists reveal distinctive binding interfaces and conformations. *EMBO J* **24:**3635–3646.

Harvey SC and Luetje CW (1996) Determinants of competitive antagonist sensitivity on neuronal nicotinic receptor β subunits. *J Neurosci* **16:**3798–3806.

Horenstein NA, McCormack TJ, Stokes C, Ren K, and Papke RL (2007) Reversal of agonist selectivity by mutations of conserved amino acids in the binding site of nicotinic acetylcholine receptors. *J Biol Chem* **282:**5899–5909.

Houlihan LM, Slater Y, Guerra DL, Peng JH, Kuo YP, Lukas RJ, Cassels BK, and Bermudez I (2001) Activity of cytisine and its brominated isosteres on recombinant human α7, α4β2 and α4β4 nicotinic acetylcholine receptors. *J Neurochem* **78:** 1029–1043.

Kuryatov A, Onksen J, and Lindstrom J (2008) Roles of accessory subunits in α4β2* nicotinic receptors. *Mol Pharmacol* **74:**132–143.

Lippiello PM, Beaver JS, Gatto GJ, James JW, Jordan KG, Traina VM, Xie J, and

Bencherif M (2008) TC-5214 (*S*-(+)-mecamylamine): a neuronal nicotinic acetylcholine receptor modulator with antidepressant activity. *CNS Neurosci Ther* **14:** 266–277.

Livingstone PD, Srinivasan J, Kew JN, Dawson LA, Gotti C, Moretti M, Shoaib M, and Wonnacott S (2009) $\alpha7$ and non-$\alpha7$ nicotinic acetylcholine receptors modulate dopamine release in vitro and in vivo in the rat prefrontal cortex. *Eur J Neurosci* **29:**539–550.

Marks MJ, Whiteaker P, Calcaterra J, Stitzel JA, Bullock AE, Grady SR, Picciotto MR, Changeux JP, and Collins AC (1999) Two pharmacologically distinct components of nicotinic receptor-mediated rubidium efflux in mouse brain require the $\beta2$ subunit. *J Pharmacol Exp Ther* **289:**1090–1103.

Moroni M, Vijayan R, Carbone A, Zwart R, Biggin PC, and Bermudez I (2008) Non-agonist-binding subunit interfaces confer distinct functional signatures to the alternate stoichiometries of the $\alpha4\beta2$ nicotinic receptor: an $\alpha4$-$\alpha4$ interface is required for Zn^{2+} potentiation. *J Neurosci* **28:**6884–6894.

Moroni M, Zwart R, Sher E, Cassels BK, and Bermudez I (2006) $\alpha4\beta2$ nicotinic receptors with high and low acetylcholine sensitivity: pharmacology, stoichiometry, and sensitivity to long-term exposure to nicotine. *Mol Pharmacol* **70:**755–768.

Morris GM, Goodsell DS, Halliday RS, Huey R, Hart WE, Belew R, and Olson AJ (1998) Automated docking using a Lamarckian genetic algorithm and empirical binding free energy function. *J Comput Chem* **19:**1639–1662.

Mukhtasimova N, Free C, and Sine SM (2005) Initial coupling of binding to gating mediated by conserved residues in muscle nicotinic receptor. *J Gen Physiol* **126:** 23–39.

Mukhtasimova N, Lee WY, Wang HL, and Sine SM (2009) Detection and trapping of intermediate states priming nicotinic receptor channel opening. *Nature* **459:**451–454.

Papke RL, Dwoskin LP, Crooks PA, Zheng G, Zhang Z, McIntosh JM, and Stokes C (2008) Extending the analysis of nicotinic receptor antagonists with the study of $\alpha6$ nicotinic receptor subunit chimeras. *Neuropharmacology* **54:**1189–1200.

Peng JH, Fryer JD, Hurst RS, Schroeder KM, George AA, Morrissy S, Groppi VE, Leonard SS, and Lukas RJ (2005) High-affinity epibatidine binding of functional, human $\alpha7$ nicotinic acetylcholine receptors stably and heterologously expressed de novo in SH-EP1 cells. *J Pharmacol Exp Ther* **313:**24–35.

Puttfarcken PS, Jacobs I, and Faltynek CR (2000) Characterization of nicotinic acetylcholine receptor-mediated [^{3}H]dopamine release from rat cortex and striatum. *Neuropharmacology* **39:**2673–2680.

Sali A and Blundell TL (1993) Comparative protein modelling by satisfaction of spatial restraints. *J Mol Biol* **234:**779–815.

Taly A, Corringer PJ, Guedin D, Lestage P, and Changeux JP (2009) Nicotinic receptors: allosteric transitions and therapeutic targets in the nervous system. *Nat Rev Drug Discov* **8:**733–750.

Thompson JD, Higgins DG, and Gibson TJ (1994) CLUSTAL W: improving the sensitivity of progressive multiple sequence alignment through sequence weighting, position-specific gap penalties and weight matrix choice. *Nucleic Acids Res* **22:**4673–4680.

Tønder JE and Olesen PH (2001) Agonists at the $\alpha4\beta2$ nicotinic acetylcholine receptors: structure-activity relationships and molecular modelling. *Curr Med Chem* **8:**651–674.

Unwin N (2005) Refined structure of the nicotinic acetylcholine receptor at 4Å resolution. *J Mol Biol* **346:**967–989.

Williams DK, Stokes C, Horenstein NA, and Papke RL (2009) Differential regulation of receptor activation and agonist selectivity by highly conserved tryptophans in the nicotinic acetylcholine receptor binding site. *J Pharmacol Exp Ther* **330:**40–53.

Xiu X, Puskar NL, Shanata JA, Lester HA, and Dougherty DA (2009) Nicotine binding to brain receptors requires a strong cation-π interaction. *Nature* **458:**534–537.

Zhong W, Gallivan JP, Zhang Y, Li L, Lester HA, and Dougherty DA (1998) From ab initio quantum mechanics to molecular neurobiology: a cation-π binding site in the nicotinic receptor. *Proc Natl Acad Sci USA* **95:**12088–12093.

Address correspondence to: Patricio Iturriaga-Vásquez, Department of Chemistry, Faculty of Sciences, University of Chile, Las Palmeras 3425, Santiago, Chile. E-mail: iturriag@uchile.cl